Turkish Journal of Electrical Engineering & Computer Sciences

http://journals.tubitak.gov.tr/elektrik/

Research Article

Turk J Elec Eng & Comp Sci
(2016) 24: 1709 – 1728

doi:10.3906/elk-1307-250

Optimal power flow by considering system security cost and small signal stability constraints

Mohammad SARVI*, **Mohammad Reza SALIMIAN**
Department of Electrical Engineering, Imam Khomeini International University, Qazvin, Iran

Received: 31.07.2013 • **Accepted/Published Online:** 29.06.2014 • **Final Version:** 23.03.2016

Abstract: The main objective of optimal power flow is to find the proper operating point for the power system. In this paper, the optimal power flow by considering system security cost (OPFSC) and the small signal stability constraint is presented. For this purpose, the total profit of the system by considering the system constraints is optimized. The total profit of the system is equal to the combination of profit from the active power consumption, active power generation cost, and system security cost. System security cost includes the cost of load shedding, which is computed for all contingencies that may occur in the system. One of the system constraints is the small signal stability constraint. The small signal stability constraint causes increasing of the small signal stability margin of the system. In this paper, a hybrid genetic algorithm and PSO (HGAPSO)-based method for performing OPFSC is presented. The proposed method is then tested on the WSCC 9-bus system. The results of the proposed method are compared with the primal-dual interior point (PDIP) method. The total profit of the system obtained from HGAPSO is better than the results of PDIP and system constraints are not completely satisfied in the results obtained from PDIP.

Key words: Optimal power flow, small signal stability, power system security, hybrid genetic algorithm, particle swarm optimization

1. Introduction

In a power system, the generation must be enough for supplying the loads of the system and the system constraints must be satisfied. The system constraints should also be able to be satisfied after the occurrence of a contingency and the system must be stable against small disturbances. For this purpose, control variables of the system such as generator active power should be adjusted. Optimal power flow (OPF) can be used for adjusting the control variables of the system.

Several methods for performing OPF are reported in the literature. Linear programming [1,2], nonlinear programming [3–8], and the interior point method [9–11] were presented for performing OPF. These optimization methods start to search for an optimum solution from one point in the search space and continue searching from one point to another point. If the initial starting point is not suitable, these methods may diverge.

The GA [12–15], PSO [16–18], ant colony [19], gravitational search algorithm [20], and artificial bee colony [21,22] methods were presented in some studies. These methods start to search for an optimum solution with a set of points that are scattered in the search space. Therefore, the probability of finding a false optimum point is less than in point-to-point optimization methods. These methods are easier than numerical calculation methods. The small signal stability constraint was not considered in above papers.

*Correspondence: sarvi@ikiu.ac.ir

In [23,24], the primal-dual interior point (PDIP) method was presented for performing OPF by considering system security cost and the small signal stability constraint. This method is complex and does not completely satisfy the system constraints.

In this paper, a hybrid genetic algorithm and PSO (HGAPSO)-based method for OPF by considering system security cost (OPFSC) by considering the small signal stability constraint and maximizing the total profit of the system is proposed. The small signal stability constraint causes an increase in the stability of the system against small disturbances.

This paper is organized as follow: in Section 2 small signal stability calculations are detailed. In Section 3 the HGAPSO algorithm is described. In Section 4 the OPFSC problem is detailed. The proposed algorithm is described in Section 5. In Section 6 characteristics of the test system are presented. Simulation results are presented in Section 7. In Section 8 results of the proposed method are compared with the PDIP method. Conclusions of this paper are presented in Section 9.

2. Small signal stability

The power system is modeled as the set of differential and algebraic equations in small signal stability calculations.

$$\dot{x} = f(xy) \tag{1}$$

$$= g(xy) \tag{2}$$

Here, f is the differential equations, x is the state variables, g is the algebraic equations, and $y$is the algebraic variables. The differential and algebraic equations of the system must be linearized around the steady-state operating point.

$$\begin{bmatrix} \Delta\dot{x} \\ 0 \end{bmatrix} = \begin{bmatrix} f_x & f_y \\ g_x & g_y \end{bmatrix} \begin{bmatrix} \Delta x \\ \Delta y \end{bmatrix} \tag{3}$$

The state matrix is computed as follows.

$$A_s = f_x - f_y g_y^{-1} g_x \tag{4}$$

We can compute the right-most system eigenvalue (system critical eigenvalue) from the state matrix [25]. If the real part of the right-most system eigenvalue is negative, the system is stable against the small disturbances. The smaller the real parts of system eigenvalues, the more stable the system is.

3. Hybrid GA and PSO (HGAPSO)

HGAPSO is combination of the GA and PSO. PSO is used instead of mutation in the GA. The PSO algorithm changes the position of population members by Eqs. (5) and (6). A flowchart of minimizing the objective function by HGAPSO is shown in Figure 1.

$$X_j^n = X_j^{n-1} + vel_j^n \tag{5}$$

$$vel_j^n = w_n \times vel_j^{n-1} + c \times R \otimes (X_{Gbest}^{n-1} - X_j^{n-1}) \tag{6}$$

Here, w_n is the inertia of the nth generation, which is changed from 0.9 to 0.4; X_j^n is the position of the jth member of the nth generation; X_{Gbest}^{n-1} is the best member of the (n – 1)th generation; c is a constant, which is considered as 2; and R is a random vector, the components of which are between 0 and 1.

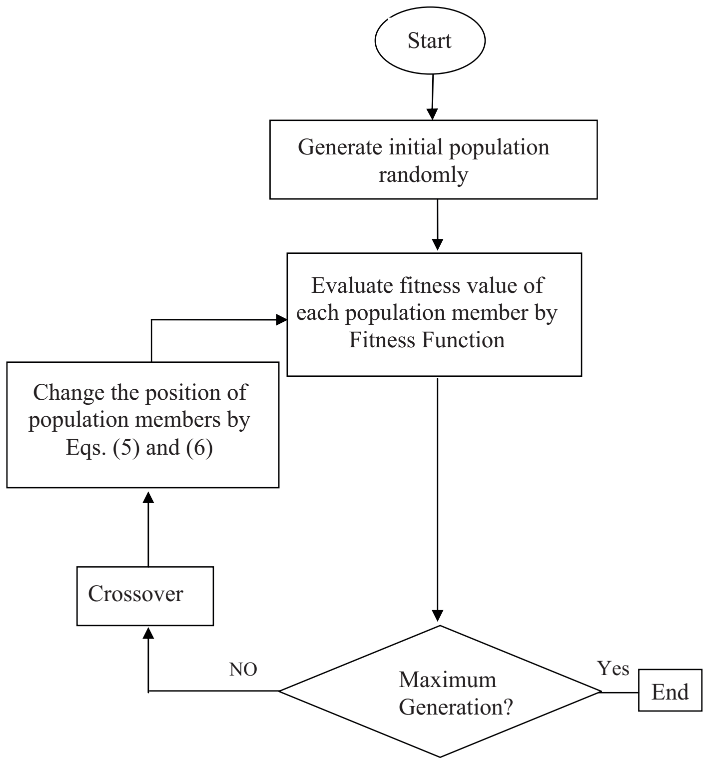

Figure 1. Flowchart of minimizing fitness function by HGAPSO

4. Description of OPFSC problem and constraints

In order to perform OPF by considering the system security cost, the total profit (TP) of the system should be maximized. Total profit of the system is computed as:

$$TP = P^0 * PR^0 + \sum_{m=1}^{M} P^m * PR^m \,, \tag{7}$$

where P^0 is:

$$P^0 = 1 - \sum_{m=1}^{M} P^m. \tag{8}$$

M is the number of contingencies that may occur in the system, P^0 is the probability of no occurring contingency in the system, P^m is the probability of the mth occurring contingency in the system, PR^0 shows the profit of the system in the precontingency state, and PR^m shows the profit of the system in the mth postcontingency state.

The profit of the system in precontingency state is computed as follows.

$$PR^0 = \sum_{i \in B_G^0} L_{Pj}(P_{L_j}^0) - \sum_{i \in B_G^0} G_{c_i}(P_{G_i}^0) \tag{9}$$

$$G_{c_i}(P_{G_i}^0) = a_{G_i} * (P_{G_i}^0)^2 + b_{G_i} * (P_{G_i}^0) + c_{G_i} \quad i \in B_G^0 \tag{10}$$

$$L_{Pj}\left(P_{L_j}^0\right) = a_{L_j} * \left(P_{L_j}^0\right)^2 + b_{L_j} * \left(P_{L_j}^0\right) + c_{L_j} \quad j \in B_L^0 \tag{11}$$

Here, $G_{c_i}(P_{G_i}^0)$ is the generator cost curve of bus i, $L_{Pj}(P_{L_j}^0)$ is the consumer profit curve of bus j, B_G^0 is the set of indices of buses that have generators in the precontingency state and B_L^0 is the set of indices of buses that have loads in the precontingency state, $P_{G_i}^0$ is the active power of bus i generator in the precontingency state, and $P_{L_j}^0$ is the active power of bus j load in the precontingency state. a_{G_i}, b_{G_i}, and c_{G_i} are the constant coefficients of the generator cost curve of bus i and a_{L_j}, b_{L_j}, and c_{L_j} are the constant coefficients of the consumer profit curve of bus j.

The profit of the system in the postcontingency state is computed as follows.

$$\sum_{j\in B_L^m}\sum_{i\in B_G^m}\sum_{j\in B_L^m} PR^m = L_{Pj}(P_{L_j}^m) - G_{c_i}(P_{G_i}^m) - L_{c_j}(P_{L_j}^0, P_{L_j}^m) \quad \text{for} \quad m = 1, ..., M \tag{12}$$

$$L_{c_j}(P_{L_j}^0, P_{L_j}^m) = b_{c_j} * (P_{L_j}^0 - P_{L_j}^m) \qquad j \in B_L^m \quad \text{for} \quad m = 1, ..., M \tag{13}$$

Here, $P_{G_i}^m$ is the active power of bus i generator in the mth postcontingency state, $P_{L_j}^m$ is the active power of the bus j load in the mth postcontingency state, $L_{c_j}(P_{L_j}^0, P_{L_j}^m)$ is the cost of load shedding in bus j, B_L^m is the set of indices of buses that have loads in the mth postcontingency state, and b_{c_j} is the constant coefficient of the cost of load shedding in bus j.

4.1. Constraints

The constraints consist of equality and inequality constraints. Equality constraints consist of load flow equations and reactive power limits of loads. Inequality constraints consist of active power limits of generators, reactive power limits of generators, active power limits of loads, voltage limits of buses, transmission power limits of lines, and the small signal stability constraint. OPFSC variables consist of voltage of buses, active and reactive power of generators and loads, and system eigenvalues, which are obtained from optimization, load flow, and small signal stability calculations. These variables must be in the permitted range. Constraints of the OPFSC are as follows.

4.1.1. Load flow equations

Load flow equations should be satisfied in precontingency and postcontingency states of the system. Thus, we have the following.

$$\sum_{k\in B_T^m} P_{G_i}^m - P_{L_i}^m = V_{B_i}^m V_{B_k}^m Y_{ik}^m cos\left(\theta_i^m - \theta_k^m - \alpha_{ik}^m\right) \quad i \in B_T^m \quad \text{for} \quad m = 0, ..., M \tag{14}$$

$$\sum_{k\in B_T^m} Q_{G_i}^m - Q_{L_i}^m = V_{B_i}^m V_{B_k}^m Y_{ik}^m sin(\theta_i^m - \theta_k^m - \alpha_{ik}^m), \quad i \in B_T^m \quad \text{for} \quad m = 0, ..., M \tag{15}$$

Here, $V_{B_i}^m\angle\theta_i^m$ is the voltage of bus i, B_T^m is the set of indices of buses, $Q_{L_i}^m$ is the reactive power of the bus i generator, $Y_{ii}^m\angle\alpha_{ii}^m$ is the sum of admittances connected to bus i, and $Y_{ik}^m\angle\alpha_{ik}^m$ is the negative value of the sum of admittances connected between bus i and $k\,(i \neq k)$.

4.1.2. Active power limits of generators

The active power of each generator must be in the allowed range in the precontingency state of the system. This limit is as follows.

$$P^0_{GMin_i} \leq P^0_{G_i} \leq P^0_{GMax_i} \quad i \in B^0_G \tag{16}$$

Here, $P^0_{GMax_i}$ and $P^0_{GMin_i}$ are the maximum and minimum allowed values for the active power of the bus i generator in the precontingency state, respectively.

The active power of each generator can be changed in the allowable range in the postcontingency state of the system. Thus, we have the following.

$$P^m_{GMin_i} \leq P^m_{G_i} \leq P^m_{GMax_i} \quad i \in B^m_G \quad \text{for} \quad m = 1, ..., M \tag{17}$$

$$P^m_{GMax_i} = min(P^0_{G_i} + \Delta_{UP} P_{G_i}\,,\, P^0_{GMax_i}) \quad i \in B^m_G \quad \text{for} \quad m = 1, ..., M \tag{18}$$

$$P^m_{GMin_i} = max\left(P^0_{G_i} - \Delta_{Down} P_{G_i}\,, P^0_{GMin_i}\right) \quad i \in B^m_G \quad \text{for} \quad m = 1, ..., M \tag{19}$$

Here, $\Delta_{UP} P_{G_i}$ is the maximum permitted value for increasing the active power of the bus i generator in the postcontingency state, and $\Delta_{Down} P_{G_i}$ is the maximum permitted value for decreasing the active power of the bus i generator in the postcontingency state.

4.1.3. Reactive power limits of generators

The reactive power of each generator is variant and must be in the permitted range in precontingency and postcontingency states of the system.

$$Q_{GMin_i} \leq Q^m_{G_i} \leq Q_{GMax_i} \quad i \in B^m_G \;\; for \quad m = 0, ..., M \tag{20}$$

Here, Q_{GMax_i} shows the maximum permitted value for the reactive power of the bus i generator, and Q_{GMin_i} shows the minimum permitted value for the reactive power of the bus i generator.

4.1.4. Active power limits of loads

The active power of each load must be in the permitted range in the precontingency state of the system.

$$P^0_{LMin_j} \leq P^0_{L_j} \leq P^0_{LMax_j} \quad j \in B^0_L \tag{21}$$

Here, $P^0_{LMax_j}$ is the maximum permitted value for the active power of the bus j load in the precontingency state, and $P^0_{LMin_j}$ is the minimum permitted value for the active power of the bus j load in the precontingency state.

Active power of each load must be in the allowable range in the postcontingency state of the system.

$$P^m_{LMin_j} \leq P^m_{L_j} \leq P^m_{LMax_j} \quad j \in B^m_L \quad \text{for} \quad m = 1, ..., M \tag{22}$$

$$P^m_{LMax_j} = P^0_{L_j} \quad j \in B^m_L \quad \text{for} \quad m = 1, ..., M \tag{23}$$

$$P^m_{LMin_j} = P^0_{LMin_j}\, j \in B^m_L \qquad \text{for} \quad m = 1, ..., M \tag{24}$$

4.1.5. Reactive power limits of loads

Reactive power of each load is a function of active power of that load in precontingency and postcontingency states of the system. This function is as follows:

$$Q_{L_j}^m = P_{L_j}^m * \frac{\sqrt{1 - pf_j^2}}{pf_j} \quad j \in B_L^m \quad \text{for} \quad m = 0, ..., M, \tag{25}$$

where pf_j shows the power factor of the bus j load.

4.1.6. Voltage limits of buses

The voltage magnitude of each bus must be in the allowable range in precontingency and postcontingency states of the system. This range is defined as follows:

$$V_{BMin_k} \leq V_{B_k}^m \leq V_{BMax_k} \quad k \in B_T^m \quad \text{for} \quad m = 0, ..., M, \tag{26}$$

where $V_{B_k}^m$ shows the voltage magnitude of bus k, V_{BMin_k} shows the minimum permitted value for the voltage magnitude of bus k, and V_{BMax_k} shows the maximum permitted value for the voltage magnitude of bus k.

4.1.7. Transmission power limits of lines

The transmission power of each line must be equal to or smaller than the maximum allowable value in precontingency and postcontingency states of the system.

$$S_{L_t}^m \leq S_{LMax_t} \quad t \in L_T^m \quad \text{for} \quad m = 0, ..., M \tag{27}$$

Here, $S_{L_t}^m$ shows the transmission power of line t, L_T^m shows the set of indices of lines, and S_{LMax_t} shows the maximum permitted value for the transmission power of line t.

4.1.8. Small signal stability constraint

The real part of the right-most eigenvalue of the system must be equal to or smaller than the maximum permitted value in precontingency and postcontingency states of the system.

$$p_{R_{right}}^m \leq p_{RMax} \quad m = 0, ..., M \tag{28}$$

Here, $p_{R_{right}}^m$ shows the real part of the right-most system eigenvalue, and p_{RMax} shows the maximum permitted value for the real part of the right-most system eigenvalue.

5. Proposed OPFSC method

In this paper OPFSC is performed by HGAPSO. For this purpose, a fitness function should be defined for the variables of the OPFSC problem. The control variables of the OPFSC problem are defined as:

$$X = [P_{G0}^0 \, P_{L0}^0 V_B^0, \, P_{G0}^1 \, P_{L0}^1 V_B^1, \, \ldots P_{G0}^M \, P_{L0}^M V_B^M], \tag{29}$$

where P_{G0}^0 is a vector that contains the initial values of generator active power in the precontingency state (G symbolizes the initial values of generators' active power), P_{L0}^0 is a vector that contains the initial values of load active power in the precontingency state (L symbolizes the initial values of loads' active power), and V_B^0 is a vector that contains the voltage magnitude of buses that have generators in the precontingency state.

The noncontrol variables consist of nongenerator buses' voltage, reactive power of generators, transmission power of lines, and system eigenvalues, which are obtained from load flow and small signal stability calculations.

The fitness value of vector X is computed by the following eight steps:

Step 1: set $m = 0$.

Step 2: if the loads' and generators' active powers exceed their constraints, change them.

$$P_{G1_i}^m = \begin{cases} P_{G0_i}^m & P_{GMin_i}^m \leq P_{G0_i}^m \leq P_{GMax_i}^m \\ P_{GMax_i}^m & P_{G0_i}^m > P_{GMax_i}^m \\ P_{GMin_i}^m & P_{G0_i}^m < P_{GMin_i}^m \end{cases} \quad \text{for } i \in B_G^m \tag{30}$$

$$P_{L1_j}^m = \begin{cases} P_{L0_j}^m & P_{LMin_j}^m \leq P_{L0_j}^m \leq P_{LMax_j}^m \\ P_{LMax_j}^m & P_{L0_j}^m > P_{LMax_j}^m \\ P_{LMin_j}^m & P_{L0_j}^m < P_{LMin_j}^m \end{cases} \quad \text{for } \ j \in B_L^m \tag{31}$$

Step 3: if $\sum\limits_{j\in B_L^m} \sum\limits_{i\in B_G^m} \sum\limits_{j\in B_L^m} (P_{LMin_j}^m \leq P_{G1_i}^m \leq P_{LMax_j}^m)$

$$P_{G2}^m = P_{G1}^m \tag{32}$$

$$P_{L2}^m = P_{L1}^m \tag{33}$$

elseif $\sum\limits_{i\in B_G^m} \sum\limits_{j\in B_L^m} (P_{G1_i}^m > P_{LMax_j}^m)$

$$\sum_{i\in B_G^m} \sum_{i\in B_G^m} \sum_{j\in B_L^m} P_{G2_i}^m = P_{G1_i}^m - \frac{(P_{G1_i}^m - P_{GMin_i}^m)}{(P_{G1_i}^m - P_{GMin_i}^m)} * (P_{G1_i}^m - P_{LMax_j}^m) \qquad \text{for } i \in B_G^m \tag{34}$$

$$P_{L2}^m = P_{L1}^m \tag{35}$$

elseif $\sum\limits_{i\in B_G^m} \sum\limits_{j\in B_L^m} (P_{G1_i}^m < P_{LMin_j}^m)$

$$\sum_{i\in B_G^m} \sum_{j\in B_L^m} \sum_{i\in B_G^m} P_{G2_i}^m = P_{G1_i}^m + \frac{(P_{GMax_i}^m - P_{G1_i}^m)}{(P_{GMax_i}^m - P_{G1_i}^m)} * (P_{LMin_j}^m - P_{G1_i}^m) \qquad \text{for } i \in B_G^m \tag{36}$$

$$P_{L2}^m = P_{L1}^m \tag{37}$$

Step 4: if $\sum\limits_{j\in B_L^m} \sum\limits_{i\in B_G^m} (P_{L2_j}^m = P_{G2_i}^m)$

$$P_G^m = P_{G2}^m \tag{38}$$

$$P_L^m = P_{L2}^m \tag{39}$$

elseif $\sum\limits_{j\in B_L^m}\sum\limits_{i\in B_G^m}(P_{L2_j}^m > P_{G2_i}^m)$

$$P_G^m = P_{G2}^m \tag{40}$$

$$\sum_{j\in B_L^m}\sum_{j\in B_L^m}\sum_{i\in B_G^m} P_{L_j}^m = P_{L2_j}^m - \frac{(P_{L2_j}^m - P_{LMin_j}^m)}{(P_{L2_j}^m - P_{LMin_j}^m)} * \left(P_{L2_j}^m - P_{G2_i}^m\right) \qquad \text{for } j \in B_L^m \tag{41}$$

elseif $\sum\limits_{j\in B_L^m}\sum\limits_{i\in B_G^m}(P_{L2_j}^m < P_{G2_i}^m)$

$$P_G^m = P_{G2}^m \tag{42}$$

$$\sum_{j\in B_L^m}\sum_{i\in B_G^m}\sum_{j\in B_L^m} P_{L_j}^m = P_{L2_j}^m + \frac{(P_{LMax_j}^m - P_{L2_j}^m)}{(P_{LMax_j}^m - P_{L2_j}^m)} * \left(P_{G2_i}^m - P_{L2_j}^m\right) \qquad \text{for } j \in B_L^m \tag{43}$$

Step 5: if $m = 0$, perform load flow and small signal stability calculations for the precontingency state; otherwise, perform load flow and small signal stability calculations for the mth postcontingency state.

Step 6: compute the value of exceeding constraints by a penalty function (Eq. (44)).

$$\begin{aligned} PF^m \quad = \quad & K_{PG} * \Delta_{limit} P_{G_{slack}}^m + K_{QG} * \sum_{i\in B_G^m} \Delta_{limit} Q_{G_i}^m \\ & + K_V * \sum_{k\in B_T^m} \Delta_{limit} V_{B_k}^m + K_S * \sum_{t\in B_T^m} \Delta_{limit} S_{L_t}^m + K_p * \Delta_{limit} p_{R_{right}}^m \end{aligned} \tag{44}$$

$$\Delta_{limit} P_{G_{slack}}^m = \begin{cases} 0 & P_{GMin_{slack}}^m \le P_{G_{slack}}^m \le P_{GMax_{slack}}^m \\ P_{G_{slack}}^m - P_{GMax_{slack}}^m & P_{G_{slack}}^m > P_{GMax_{slack}}^m \\ P_{GMin_{slack}}^m - P_{G_{slack}}^m & P_{G_{slack}}^m < P_{GMin_{slack}}^m \end{cases} \tag{45}$$

$$\Delta_{limit} Q_{G_i}^m = \begin{cases} 0 & Q_{GMin_i} \le Q_{G_i}^m \le Q_{GMax_i} \\ Q_{G_i}^m - Q_{GMax_i} & Q_{G_i}^m > Q_{GMax_i} \\ Q_{GMin_i} - Q_{G_i}^m & Q_{G_i}^m < Q_{GMin_i} \end{cases} \qquad \text{for } i \in B_G^m \tag{46}$$

$$\Delta_{limit} V_{B_k}^m = \begin{cases} 0 & V_{BMin_k} \le V_{B_k}^m \le V_{BMax_k} \\ V_{B_k}^m - V_{BMax_k} & V_{B_k}^m > V_{BMax_k} \\ V_{BMin_k} - V_{B_k}^m & V_{B_k}^m < V_{BMin_k} \end{cases} \qquad \text{for } k \in B_T^m \tag{47}$$

$$\Delta_{limit} S_{L_t}^m = \begin{cases} 0 & S_{L_t}^m \le S_{LMax_t} \\ S_{L_t}^m - S_{LMax_t} & S_{L_t}^m > S_{LMax_t} \end{cases} \qquad \text{for } t \in L_T^m \quad A_s = f_x - f_y g_y^{-1} g_x \tag{48}$$

$$\Delta_{limit} p_{R_{right}}^m = \begin{cases} 0 & p_{R_{right}}^m \le p_{RMax} \\ p_{R_{right}}^m - p_{RMax} & p_{R_{right}}^m > p_{RMax} \end{cases} \tag{49}$$

Here, $\Delta_{limit} P^m_{G_{slack}}$ shows the value of exceeding the permitted range of slack generator active power, $\Delta_{limit} Q^m_{G_i}$ shows the value of exceeding the permitted range of generator reactive power, $\Delta_{limit} V^m_{B_k}$ shows the value of exceeding the permitted range of bus voltage, $\Delta_{limit} S^m_{L_t}$ shows the value of exceeding the permitted range of the transmission power of lines, and $\Delta_{limit} p^m_{R_{right}}$ shows the value of exceeding the maximum permitted value for the real part of the right-most system eigenvalue. K_{PG} shows the penalty factor of exceeding the permitted range of slack generator active power, K_{QG} shows the penalty factor of exceeding the permitted range of generator reactive power, K_V shows the penalty factor of exceeding the permitted range of bus voltage, K_S shows the penalty factor of exceeding the permitted range of the transmission power of lines, and K_p shows the penalty factor of exceeding the maximum permitted value for the real part of the right-most system eigenvalue.

Step 7: if $m = 0$, compute the profit of the system (PR^0) by Eq. (9), else compute the profit of the system (PR^m) by Eq. (12).

Step 8: if $m \leq M$, set $m = m + 1$ and go to step 2, else compute the fitness value of vector X by Eq. (50).

$$\text{Fitness value}\,(X) = PF - TP \tag{50}$$

$$\sum_{m=0}^{M} PF = PF^m \tag{51}$$

$$\sum_{m=0}^{M} TP = P^m * PR^m \tag{52}$$

6. Test system

The WSCC 9-bus system shown in Figure 2 is used as a test system in this paper. Some properties of the test system were presented in [23,26]. Six contingencies are defined in the WSCC 9-bus system. These contingencies consist of outages of lines 4-6, 4-5, 5-7, 6-9, 7-8, and 8-9. The probability of each contingency is 0.01 $(P^m = 0.01\,,\ m = 1,\, 2, ..., 6)$. Generator data, generator cost curve coefficients, voltage limits of buses, line and transformer data, load and generator constraint data, consumer profit curve coefficients, and load shedding cost coefficients are shown in Tables 1–7, respectively. S_{base} is $100\,MVA$ $(S_{base}= 100\,MVA)$.

7. Simulation results

In order to investigate the accuracy and performance of the proposed method, a test WSCC 9-bus system is considered. The proposed method is tested on the WSCC 9-bus system for different conditions of the small signal stability constraint. The maximum permitted value for the real part of the right-most system eigenvalue is considered as 0, –0.15, –0.2, and –0.25. HGAPSO is coded by using the MATLAB Optimization Toolbox [27]. Population size, crossover fraction, and the maximum number of generations are considered as 60, 0.8, and 20, respectively.

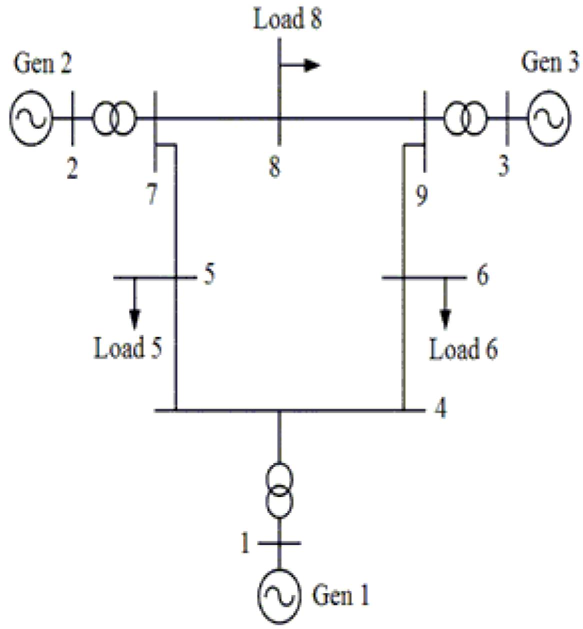

Figure 2. WSCC 9-bus system.

Table 1. Generator data.

Parameter / Generator	Gen 1	Gen 2	Gen 3
K_A	20	20	20
$T_A\,(s)$	0.2	0.2	0.2
K_E	1.0	1.0	1.0
T_E (s)	0.314	0.314	0.314
K_F	0.063	0.063	0.063
$T_F\,(s)$	0.35	0.35	0.35
$X_d\,(p.u.)$	0.146	0.8958	1.3125
$X_d^{'}\,(p.u.)$	0.0608	0.1198	0.1813
$X_q\,(p.u.)$	0.0969	0.8645	1.2547
$X_q^{'}\,(p.u.)$	0.0969	0.1969	0.25
$T_{do}^{'}(s)$	8.96	6.0	5.89
$T_{qo}^{'}(s)$	0.31	0.535	0.6
$H\,(s)$	23.64	6.4	3.01
D	0.0	0.0	0.0
$S_{Ei}(E_{fdi}) = 0.0039e^{1.555E_{fdi}}$			

Table 2. Generator cost curve coefficients.

Bus no.	$a_G\,(\$/MW^2h)$	$b_G\,(\$/MWh)$	$c_G(\$/h)$
1	8.20e-4	12.712	0.00
2	8.76e-4	12.001	0.00
3	6.46e-4	12.290	0.00

Table 3. Voltage limits of buses.

Bus no. / Parameter	1	2	3	4	5	6	7	8	9
V_{BMin} $(p.u.)$	0.950	0.955	0.955	0.955	0.955	0.955	0.955	0.950	0.955
V_{BMax} $(p.u.)$	1.04	1.045	1.045	1.09	1.09	1.09	1.09	1.09	1.09

Table 4. Line and transformer data.

Bus no.	Bus no.	R (P.U.)	X (P.U.)	Y (P.U.)	$S_{LMAX}\,(MVA)$
1	4	0.0000	0.0576	0.000	450
2	7	0.0000	0.0625	0.000	320
3	9	0.0000	0.0586	0.000	335
4	5	0.0100	0.0850	0.176	390
4	6	0.0170	0.0920	0.158	325
5	7	0.0320	0.1610	0.306	375
6	9	0.0390	0.1700	0.358	375
7	8	0.0085	0.0720	0.149	375
9	8	0.1190	0.1008	0.209	375

Table 5. Load and generator constraint data.

Bus no. / Parameter	1	2	3	4	5	6	7	8	9
$P_{GMax}\,(MW)$	250	270	285	-	-	-	-	-	-
$P_{GMin}\,(MW)$	25	25	35	-	-	-	-	-	-
$\Delta_{UP}P_G\,(MW)$	50	35	35	-	-	-	-	-	-
$\Delta_{Down}P_G\,(MW)$	50	35	35	-	-	-	-	-	-
$Q_{GMax}\,(MVAR)$	100	100	100	-	-	-	-	-	-
$Q_{GMin}\,(MVAR)$	–50	–50	–50	-	-	-	-	-	-
$P_{LMax}\,(MW)$	-	-	-	-	125	90	-	100	-
$P_{LMin}\,(MW)$	-	-	-	-	0	0	-	0	-
pf	-	-	-	-	0.928	0.948	-	0.943	-

Table 6. Consumer profit curve coefficients.

Bus no.	$a_L(\$/MW^2h)$	$b_L(\$/MWh)$	$c_L(\$/h)$
5	–0.1047	38.665	0.00
6	–0.0231	16.844	0.00
8	–0.0431	21.630	0.00

Table 7. Load shedding cost coefficients.

Bus no.	$b_c(\$/MWh)$
5	100
6	100
8	100

7.1. The proposed method's results

7.1.1. The proposed method's results with $p_{RMax} = 0$

The minimum values of the fitness function in different generations of HGAPSO are shown in Figure 3. The minimum value of the fitness function at the end of the generations is –2291.95. The results obtained from the proposed method are presented in Table 8. Total profit of system is equal to 2291.95 $(\$/h)$.

The real part of the most critical eigenvalue of the system is –0.152, created after removing line 6-9 and smaller than 0. System constraints are completely satisfied in the results obtained from the proposed method.

7.1.2. The proposed method's results with $p_{RMax} = -015$

The minimum values of the fitness function in different generations of HGAPSO are shown in Figure 4. The minimum value of the fitness function at the end of the generations is –2287.89. The results obtained from HGAPSO are presented in Table 9. Total profit of system is equal to 2287.89 $(\$/h)$.

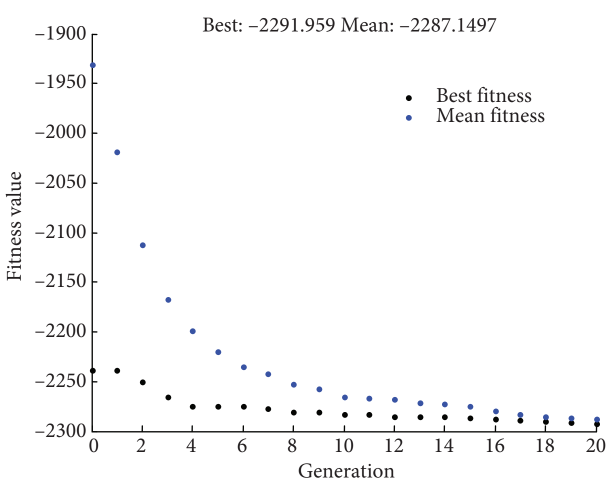

Figure 3. The minimum values of fitness function obtained from the proposed method $(p_{RMax} = 0)$.

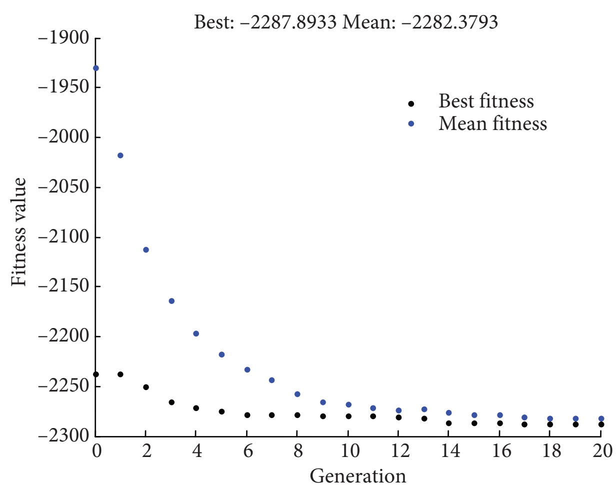

Figure 4. The minimum values of fitness function obtained from the proposed method $(p_{RMax} = -0.15)$.

The real part of the most critical eigenvalue of the system is –0.159, created after removing line 6-9 and smaller than –0.15. System constraints are completely satisfied in the results obtained from the proposed method.

7.1.3. The proposed method's results with $p_{RMax} = -02$

The minimum values of the fitness function in different generations of HGAPSO are shown in Figure 5. The minimum value of the fitness function at the end of the generations is –2281.13. The results obtained from the proposed method are presented in Table 10. Total profit of system is equal to 2281.13 $(\$/h)$.

The real part of the most critical eigenvalue of the system is –0.201, created after removing line 4-6 and smaller than –0.2. System constraints are completely satisfied in the results obtained from the proposed method.

Table 8. The results obtained from the proposed method for $p_{RMax} = 0(TP = 2291.95\,(\$/h))$.

m	State	Critical eigenvalue	P_{G_1} (MW)	P_{G_2} (MW)	P_{G_3} (MW)	P_{L_5} (MW)	P_{L_6} (MW)	P_{L_8} (MW)	V_{B_1} (P.U.)	V_{B_2} (P.U.)	V_{B_3} (P.U.)	PR ($\$/h$)
0	Precont.	–0.242 ± 8.441i	79.3971	136.951	98.4353	120.91	90	100	1.04	1.045	1.045	2314.84
1	Line 4-6	–0.235 ± 7.264i	103.914	149.772	63.4353	120.91	90	100	1.04	1.03688	1.045	2275.44
2	Line 4-5	–0.217 ± 6.709i	75.5754	130.202	91.6870	101.644	90	100	1.04	1.045	1.045	306.730
3	Line 5-7	–0.171 ± 6.232i	89.01908	135.8253	97.30967	120.91	90	100	1.04	1.045	0.955	2218.411
4	Line 6-9	–0.152 ± 7.061i	86.36294	135.8253	97.30967	120.91	90	100	1.04	1.045	0.955	2253.105
5	Line 7-8	–0.189 ± 7.742i	39.67453	160.0195	121.5039	120.91	90	100	1.04	1.045	1.044991	2254.041
6	Line 8-9	–0.297 ± 7.953i	83.2386	135.8253	97.30967	120.91	90	100	1.04	1.045	1.045	2292.71

Table 9. The results obtained from the proposed method for $p_{RMax} = -0.15\,(TP = 2287.89\,(\$/h)$.

m	State	Critical eigenvalue	P_{G_1} (MW)	P_{G_2} (MW)	P_{G_3} (MW)	P_{L_5} (MW)	P_{L_6} (MW)	P_{L_8} (MW)	V_{B_1} (P.U.)	V_{B_2} (P.U.)	V_{B_3} (P.U.)	PR ($\$/h$)
0	Precont.	–0.304 ± 8.394i	69.9905	112.0698	123.8468	119.57	82.47	100	1.04	1.045	1.045	2308.794
1	Line 4-6	–0.208 ± 7.333i	74.42307	110.1772	121.9542	119.57	82.47	100	1.04	1.041155	1.045	2298.03
2	Line 4-5	–0.243 ± 6.705i	50.40927	113.928	125.705	101.6821	82.47	100	1.04	1.045	1.045	447.2189
3	Line 5-7	–0.165 ± 6.563i	79.21619	110.1772	121.9542	119.57	82.47	100	1.04	1.045	1.044546	2236.496
4	Line 6-9	–0.159 ± 7.125i	69.33553	115.1136	126.8906	119.57	82.47	100	1.04	1.045	1.045	2242.159
5	Line 7-8	–0.295 ± 7.938i	75.67539	110.1772	121.9542	119.57	82.47	100	1.039959	1.045	1.045	2281.956
6	Line 8-9	–0.268 ±10.410i	77.6741	110.1772	121.9542	119.57	82.47	100	1.04	1.038344	1.045	2256.832

Table 10. The results obtained from the proposed method for $p_{RMax} = -0.2\,(TP = 2281.13\,(\$/h)$.

m	State	Critical eigenvalue	P_{G_1} (MW)	P_{G_2} (MW)	P_{G_3} (MW)	P_{L_5} (MW)	P_{L_6} (MW)	P_{L_8} (MW)	V_{B_1} (P.U.)	V_{B_2} (P.U.)	V_{B_3} (P.U.)	PR ($\$/h$)
0	Precont.	–0.295 ± 8.395i	76.5899	115.404	127.249	125	90	100	1.04	1.045	1.045	2308.636
1	Line 4-6	–0.201 ± 7.301i	80.28737	113.8953	126.1253	125	90	100	1.04	1.0289	1.045	2293.561
2	Line 4-5	–0.274 ± 6.649i	71.16802	107.2981	119.1431	101.4493	90	100	1.04	1.045	1.045	–129.299
3	Line 5-7	–0.243 ± 6.590i	102.4871	80.404	139.915	125	90	100	1.04	1.045	1.045	2243.049
4	Line 6-9	–0.234 ± 7.100i	103.1926	80.404	139.915	125	90	100	1.04	1.044989	1.003803	2234.728
5	Line 7-8	–0.284 ± 7.820i	81.22224	114.168	126.013	125	90	100	1.0115	1.045	1.045	2279.625
6	Line 8-9	–0.328 ± 7.907i	99.88129	128.07	92.249	125	90	100	1.0386	1.045	1.045	2289.592

7.1.4. The proposed method's results with $p_{RMax}= -025$

The minimum values of the fitness function in different generations of HGAPSO are shown in Figure 6. The minimum value of the fitness function at the end of the generations is –2274.94. The results obtained from HGAPSO are presented in Table 11. Total profit of system is equal to 2274.94 $(\$/h)$.

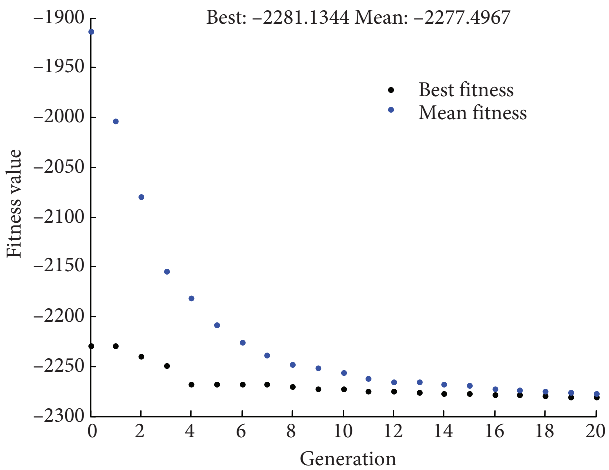

Figure 5. The minimum values of fitness function obtained from the proposed method $(p_{RMax} = -0.2)$

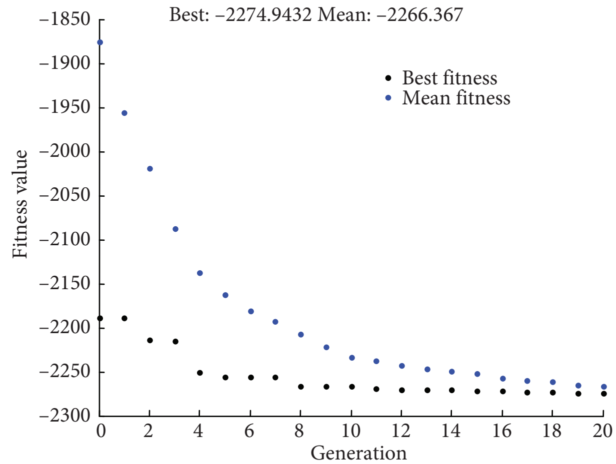

Figure 6. The minimum values of fitness function obtained from the proposed method $(p_{RMax} = -0.25)$.

The real part of the most critical eigenvalue of the system is –0.251, created after removing line 6-9 and smaller than –0.25. System constraints are completely satisfied in the results obtained from the proposed method.

8. Comparison of results of the proposed method and PDIP methods

In [23,24], OPF by considering system security cost and the small signal stability constraint was performed on the WSCC 9-bus system by the PDIP method. The results of the PDIP method are shown in Tables 12–15. The profit of the system and total profit of the system (TP) in Tables 12–15 are computed by considering load shedding cost. If we are computing the profit of the system by neglecting the load shedding cost, it becomes equal to 2192.76, 2192.33, 2170.18, and 2130.20 after removing line 4-5 in Tables 12–15, respectively. The total profit of the system (TP) becomes equal to 2314.59, 2313.45, 2307.96, and 2300.80 in Tables 12–15, respectively. The total profits of the system by considering load shedding cost obtained from the proposed method and PDIP are presented in Table 16.

As shown in Table 16, the results obtained from the proposed method are better than the results obtained from PDIP. Also, some constraints are violated in the results obtained from PDIP. For example, voltage limits of buses and active power limits of loads are violated in the results presented in Tables 12–15. The voltage values of Table 14 were not mentioned in [23,24].

The maximum permitted values for P_{L_8} and V_{B_1} are 100 MW and 1.04 P.U., respectively, but as shown in Tables 12–15, P_{L_8} and V_{B_1} are greater than the maximum permitted values.

Table 11. The results obtained from the proposed method for $p_{RMax} = -0.25\,(TP = 2274.94\,(\$/h)$.

m	State	Critical eigenvalue	P_{G_1} (MW)	P_{G_2} (MW)	P_{G_3} (MW)	P_{L_5} (MW)	P_{L_6} (MW)	P_{L_8} (MW)	V_{B_1} (P.U.)	V_{B_2} (P.U.)	V_{B_3} (P.U.)	PR ($\$/h$)
0	Precont.	–0.443 ± 0.522i	104.293	80.47267	123.5109	119.88	85.29	100	1.0377	1.045	1.045	2297.30
1	Line 4-6	–0.324 ± 7.207i	107.758	79.57128	122.6095	119.88	85.29	100	1.0381	1.045	1.045	2274.25
2	Line 4-5	–0.309 ± 6.621i	60.4692	93.9769	137.0151	99.98	85.29	100	1.04	1.045	1.04322	226.899
3	Line 5-7	–0.254 ± 6.626i	109.082	79.57128	122.6095	119.88	85.29	100	1.0336	1.045	1.045	2257.20
4	Line 6-9	–0.251 ± 7.149i	109.409	79.57128	122.6095	119.88	85.29	100	1.0177	1.045	1.045	2252.98
5	Line 7-8	–0.346 ±10.56i	107.561	79.57128	122.6095	119.88	85.29	100	1.04	0.9811	1.0422	2276.80
6	Line 8-9	–0.380 ±10.52i	128.551	93.61105	88.5109	119.88	85.29	100	1.0265	1.045	1.045	2259.56

Table 12. The results obtained from PDIP for $p_{RMax} = 0\,(TP = 2286.39\,(\$/h)$.

m	State	Critical eigenvalue	P_{G_1} (MW)	P_{G_2} (MW)	P_{G_3} (MW)	P_{L_5} (MW)	P_{L_6} (MW)	P_{L_8} (MW)	V_{B_1} (P.U.)	V_{B_2} (P.U.)	V_{B_3} (P.U.)	PR ($\$/h$)
0	Precont.	–0.1784 ± 9.5491i	66.47	161.47	82.81	117.92	83.86	104.73	1.05	1.045	1.045	2317.23
1	Line 4-6	–0.1302 ± 8.2630i	43.28	164.99	103.79	117.92	83.86	104.73	1.05	1.045	1.045	2308.03
2	Line 4-5	–0.1448 ± 7.5089i	30.52	148.32	104.24	89.72	83.86	104.73	1.05	1.045	1.045	–627.24
3	Line 5-7	–0.1266 ± 7.4864i	116.47	126.27	69.35	117.92	83.86	104.73	1.05	1.045	1.045	2266.01
4	Line 6-9	–0.1888 ± 8.0426i	115.23	147.88	47.81	117.92	83.86	104.73	1.05	1.045	1.045	2287.55
5	Line 7-8	–0.2053 ± 8.9385i	69.57	126.27	117.81	117.92	83.86	104.73	1.05	1.045	1.045	2271.64
6	Line 8-9	–0.1703 ± 9.0671i	68.57	181.47	60.89	117.92	83.86	104.73	1.05	1.045	1.045	2313.55

Table 13. The results obtained from PDIP $p_{RMax} = -0.15\,(TP = 2285.38\,(\$/h)$.

m	State	Critical eigenvalue	P_{G_1} (MW)	P_{G_2} (MW)	P_{G_3} (MW)	P_{L_5} (MW)	P_{L_6} (MW)	P_{L_8} (MW)	V_{B_1} (P.U.)	V_{B_2} (P.U.)	V_{B_3} (P.U.)	PR ($\$/h$)
0	Precont.	–0.1996 ± 9.4823i	82.08	146.93	80.84	117.77	83.84	104.81	1.05	1.045	1.045	2315.97
1	Line 4-6	–0.1508 ± 8.1927i	58.22	159.66	93.71	117.77	83.84	104.81	1.05	1.045	1.045	2306.37
2	Line 4-5	–0.1525 ± 7.4783i	38.96	146.28	97.65	89.70	83.84	104.81	1.05	1.045	1.045	–614.67
3	Line 5-7	–0.1504 ± 7.3542i	132.08	111.93	67.10	117.77	83.84	104.81	1.03	1.045	1.045	2269.74
4	Line 6-9	–0.1941 ± 8.0361i	115.34	149.62	45.84	117.77	83.84	104.81	1.05	1.045	1.045	2287.78
5	Line 7-8	–0.2426 ± 8.8572i	84.77	111.93	115.84	117.77	83.84	104.81	1.05	1.045	1.045	2274.78
6	Line 8-9	–0.1793 ± 9.0672i	68.47	181.49	60.87	117.77	83.84	104.81	1.05	1.045	1.045	2313.18

Table 14. The results obtained from PDIP $p_{RMax} = -0.2\,(TP = 2279.75\,(\$/h)$.

m	State	Critical eigenvalue	P_{G_1} (MW)	P_{G_2} (MW)	P_{G_3} (MW)	P_{L_5} (MW)	P_{L_6} (MW)	P_{L_8} (MW)	PR (P.U.)
0	Precont.	–0.2395 ± j’9.3605	101.85	128.17	79.15	117.55	83.86	104.90	2310.54
1	Line 4-6	–0.2002 ± J8.0186	83.91	150.62	76.85	117.55	83.86	104.90	2294.92
2	Line 4-5	–0.2007 ± j’7.2663	80.75	135.91	66.02	89.34	83.86	104.90	–650.82
3	Line 5-7	–0.2002 ± j’7.2127	151.85	93.17	64.92	117.55	83.86	104.90	2267.58
4	Line 6-9	–0.2040 ± j’8.0177	120.91	145.34	44.15	117.55	83.86	104.90	2287.54
5	Line 7-8	–0.2968 ± j’8.7305	100.08	97.36	114.15	117.55	83.86	104.90	2274.66
6	Line 8-9	–0.2000 ± j’9.9721	90.35	161.99	57.66	117.55	83.86	104.90	2310.09

Table 15. The results obtained from PDIP $p_{RMax} = -0.25\,(TP = 2272.11(\$/h)$.

m	State	Critical eigenvalue	P_{G_1} (MW)	P_{G_2} (MW)	P_{G_3} (MW)	P_{L_5} (MW)	P_{L_6} (MW)	P_{L_8} (MW)	V_{B_1} (P.U.)	V_{B_2} (P.U.)	V_{B_3} (P.U.)	PR ($\$/h$)
0	Precont.	–0.2809 ± j'9.2405	116.67	114.19	77.92	117.37	83.88	104.95	1.05	1.045	1.045	230(P.U.).84
1	Line 4-6	–0.2503 ± j'7.7805	103.72	145.36	62.66	117.37	83.88	104.95	1.039	1.045	1.045	2278.57
2	Line 4-5	–0.2506 ± j'7.0335	114.23	126.28	42.92	88.68	83.88	104.95	1.05	1.045	1.045	–738.80
3	Line 5-7	–0.2503 ± j'7.0745	166.67	79.19	63.58	117.37	83.88	104.95	1.03	1.045	1.045	2260.13
4	Line 6-9	–0.2513 ± j'8.8616	155.18	111.13	42.92	117.37	83.88	104.95	1.05	1.045	1.045	2275.92
5	Line 7-8	–0.2963 ± j'8.7323	101.13	97.45	112.92	117.37	83.88	104.95	1.05	1.045	1.045	2273.69
6	Line 8-9	–0.2500 ± j'8.7992	114.44	140.67	54.36	117.37	83.88	104.95	1.05	1.045	1.045	2300.47

Table 16. Total profit of the system by considering the cost of load shedding.

p_{RMax}	TP_{HGAPSO} ($\$/h$)	TP_{PDIP} ($\$/h$)
0	2291.95	2286.39
–0.15	2287.89	2285.38
–0.20	2281.13	2279.75
–0.25	2274.94	2272.11

9. Conclusion

In this paper, a HGAPSO-based method has been presented for performing OPFSC. The presented method was tested on the WSCC 9-bus system for different conditions of the small signal stability constraint. System constraints were completely satisfied in the proposed method. Therefore, OPFSC with small signal stability constraints can be performed by the proposed method.

The results obtained from the proposed method and PDIP were compared with each other. The total profits of the system obtained from the proposed method are better than the results of PDIP. Also, system constraints are not completely satisfied in the results obtained from PDIP.

The proposed method was implemented by a DELL PC (2.66 GHz CPU). The computation time is about 30 min. For decreasing the computation time, we could perform OPF separately for each contingency and use a parallel processor, which is suitable for performing the HGAPSO algorithm.

References

[1] Wells DW. Method for economic secure loading of a power system. Proc IEEE 1968; 115: 606-614.

[2] Stott B, Hobson E. Power system security control calculation using linear programming. IEEE T Power Ap Syst 1978; 97: 1713-1731.

[3] Dommel HW, Tinny WF. Optimal power flow solution. IEEE T Power Ap Syst 1968; 87: 1866-1876.

[4] Sasson AM. Combined use of parallel and Fletcher-Powell non-linear programming method for optimal load flows. IEEE T Power Ap Syst 1969; 88: 1530-1537.

[5] Alsac O, Stort B. Optimal load flow with steady state security. IEEE T Power Ap Syst 1974; 93: 745-754.

[6] Barcelo WR, Lemmon WW, Koen HR. Optimization of the real-time dispatch with constraints for secure operation of bulk power systems. IEEE T Power Ap Syst 1977; 96: 741-757.

[7] Rehn CJ, Bubenko JA, Sjelvgven D. Voltage optimization using augmented Lagrangian functions and quasi-Newton techniques. IEEE T Power Syst 1989; 4: 1470-1483.

[8] Habiabollahzadeh H, Luo GX, Semlyen A. Hydrothermal optimal power flow based on a combined linear and non-linear programming methodology. IEEE T Power Syst 1989; 4: 530-537.

[9] Momoh JA, Austin RA, Adapa R. Feasibility of interior point method for VAR planning. In: North American Power Symposium; 1992.

[10] Momoh JA, Guo SX, Ogbuobiri CE, Adapa R. The quadratic interior point method for solving power system optimization problems. In: IEEE/PES Summer Meeting; 1993. Paper No. 93 SM 4T5-BC.

[11] Lu NC, Unum MR. Network constrained security control using an interior point algorithm. In: IEEE/PES Summer Meeting; 1992.

[12] Chen PH, Chang HC. Large-scale economic dispatch by genetic algorithm. IEEE T Power Syst 1995; 10: 1919-1926.

[13] Devaraj D, Yegnanarayana B. Genetic-algorithm-based optimal power flow for security enhancement. IEE P-Gener Transm D 2005; 152: 899-905.

[14] Kumari MS, Maheswarapu S. Enhanced genetic algorithm based computation technique for multi-objective optimal power flow solution. Int J Elec Power 2010; 32: 736-742.

[15] Chan KY, Ling SH, Chan KW, Iu HHC, Pong GTY. Solving multi-contingency transient stability constrained optimal power flow problems with an improved GA. In: IEEE Congress on Evolutionary Computation; 2007. pp. 2901-2908.

[16] Mo N, Zou ZY, Chan KW, Pong TYG. Transient stability constrained optimal power flow using particle swarm optimization. IET Gener Transm Dis 2007; 1: 476-483.

[17] Park JB, Lee KS, Shin JR, Lee KY. A particle swarm optimization for economic dispatch with nonsmooth cost functions. IEEE T Power Syst 2005; 20: 34-41.

[18] Yumbla PEO, Ramirez JM, Coello CA. Optimal power flow subject to security constraints solved with a particle swarm optimizer. IEEE T Power Syst 2008; 23: 33-40.

[19] Yuan-Kang W. Resolution of the unit commitment problems by using the hybrid Taguchi-ant colony system algorithm. Int J Elec Power 2013; 49: 188-198.

[20] Duman S, Güvenç U, Sönmez Y, Yörükeren N. Optimal power flow using gravitational search algorithm. Energ Convers Manage 2012; 59: 86-95.

[21] Ayan K, Kılıç U. Solution of transient stability-constrained optimal power flow using artificial bee colony algorithm. Turk J Electr Eng Co 2013; 21: 360-372.

[22] Adaryani MR, Karami A. Artificial bee colony algorithm for solving multi-objective optimal power flow problem. Int J Elec Power 2013; 53: 219-230.

[23] Condren J, Gedra TW. Expected-security cost optimal power flow with small-signal stability constraints. IEEE T Power Syst 2006; 21: 1736-1743.

[24] Condren J. Expected-security-cost optimal power flow with small-signal stability constraints. PhD, Oklahoma State University, Stillwater, OK, USA, 2003.

[25] Lehoucq RB, Sorensen DC, Yang C. ARPACK Users' Guide: Solution of Large-Scale Eigenvalue Problems with Implicitly Restarted Arnoldi Methods. Philadelphia, PA, USA: SIAM Publications, 1998.

[26] Sauer PW, Pai M. Power System Dynamics and Stability. Upper Saddle River, NJ, USA: Prentice Hall, 1998.

[27] MathWorks. MATLAB Optimization Toolbox User's Guide, Version 7.6. Natick, MA, USA: MathWorks Inc., 2008.